Direct Observational Evidence from Space of the Effect of CO_2 Increase on Longwave Spectral Radiances: The Unique Role of High Spectral Resolution Measurements

João Teixeira[1], Robert C. Wilson[1], Heidar Th. Thrastarson[1]

[1]Jet Propulsion Laboratory, California Institute of Technology, Pasadena, California, 91109, USA

Correspondence to: Joao Teixeira (teixeira@jpl.nasa.gov)

Abstract. We present a direct measurement of the impact of increased atmospheric CO_2 on the spectra of Earth's longwave radiation obtained from space. The goal of this study is to experimentally confirm that the direct effects of CO_2 increase on the Earth's outgoing longwave spectra follow theoretical estimates, by developing a methodology that allows for a direct and more precise comparison between theory and observations. In this methodology, a search is performed to find selected ensembles of observed atmospheric vertical profiles of temperature and water vapor that are as close as possible to each other in terms of their values. By analysing the spectral radiances measured from space by the Atmospheric Infrared Sounder (AIRS), corresponding to the selected ensembles of profiles, the effects of increased CO_2 on the spectra can be isolated from the temperature and water vapor effects. The results illustrate the impact of the increase of CO_2 on the longwave spectra and compare well with theoretical estimates. As far as the authors are aware, this is the first time that the spectral signature of the increase of CO_2 (isolated from temperature and water vapor changes) has been directly observed from space.

1 Introduction

As is clearly discussed in the excellent historical compilation of Archer and Pierrehumbert (2011), and the essential references therein, it has been known for decades that an increase of atmospheric greenhouse gases such as CO_2 can lead to global warming essentially by changing the longwave radiative fluxes of energy at the top of the atmosphere. While remarkable progress has been made over the last few decades in laboratory, theoretical, modelling and prediction studies of the physics of climate change (e.g., Plass, 1956; Manabe and Wetherald, 1967, 1975; Hansen et al., 1984; Ramanathan, 1988; Ramaswamy et al., 2018), the experimental confirmation from space of the direct effects of CO_2 (independent from temperature and water vapor changes) on the Earth's outgoing longwave spectra has been elusive. The goal of the present study is to experimentally confirm that the direct effects of CO_2 increase on the Earth's outgoing longwave spectra follow theoretical estimates, by developing a methodology that allows for a direct and more precise comparison between theory and observations.

Kiehl (1983) discussed the possibility of utilizing spectrally resolved satellite measurements of longwave radiation to detect and characterize the impact of climate change on the longwave spectra, and simulated the changes in clear-sky spectra due to

increases in CO_2 and temperature. This pioneering modelling study has been followed by other modelling studies focused on the spectral signature of climate change (e.g., Mlynczak et al., 2016; Brindley and Bantges, 2016).

The fact that measurements from space of the direct effects of increased CO_2 on the longwave spectra have been notoriously difficult to obtain is associated with the sparsity of high spectral resolution observations of longwave radiances before the early 21st century and with the challenge of disentangling the effects of CO_2, temperature, and water vapor on the spectral radiances. While measurements of the spectral effects of the combined changes in CO_2, temperature, water vapor and other gases have been published (e.g., Harries et al., 2001; Brindley and Bantges, 2016; Strow and DeSouza-Machado, 2020; Whitburn et al., 2021; Huang et al., 2022), the direct effects of CO_2 alone have been difficult to depict accurately.

For example, in a pioneering study, Harries et al. (2001) calculated the spectral differences between two infrared instruments, one launched in the 1970s and the other in the 1990s. Despite the difficulties of accurately estimating spectral differences between two different instruments, Harries et al. (2001) are able to discern and potentially assign, using model simulations, some of the spectral differences to changes in greenhouse gases such as CO_2. However, they do not attempt to disentangle the effects due purely to CO_2, from temperature and water vapor changes, in the observational data. In a recent study, De Longueville et al. (2021) illustrate the increased CO_2 absorption in the Infrared Atmospheric Sounding Interferometer (IASI) spectra from 2008 to 2017, although they do not isolate it from the joint effects of temperature and water vapor.

The recent studies of Strow and DeSouza-Machado (2020) and Huang et al. (2022) investigate in detail the AIRS instrument radiance trends over the last several years and highlight the remarkable stability of the AIRS radiance record, while also discussing the role of temperature, water vapor, CO_2, and other gases in framing the nature of the AIRS radiances. However, they only isolate these effects using modelling/theoretical approaches. These studies do not attempt to disentangle the impact of CO_2 (or other gases) from temperature and water vapor in the observational data directly.

In the present study, a new methodology is proposed for a more direct measurement of the effect of CO_2 increase on longwave spectral radiances in such a way as to provide a direct and more precise comparison to theoretically derived radiances. The goal of this approach is to isolate the effects of CO_2 from the effects of temperature and water vapor. This is achieved by searching for atmospheric profiles of temperature and water vapor that are as close to each other as possible (referred to as analogues), but that have CO_2 concentrations that are significantly different. Measuring from space the spectral radiances that correspond to these analogues allows to detect, given the right circumstances, the unique impact of CO_2 on the radiances with enough precision and accuracy in key spectral regions. Specifically, in this work, 1000 temperature and water vapor reference profiles are selected and a search is performed for analogue profiles that are close to the reference profiles to within a specified uncertainty range.

Formatted: Font color: Red, English (US)

Deleted: Given the steady increase of global CO_2, the best way to make sure that analogues with significantly different values of CO_2 are selected, is to search for these analogues over several

2 Observational Data

The spectral longwave radiances are measured by the Atmospheric Infrared Sounder (AIRS), and the profiles of atmospheric temperature and water vapor, as well as cloud properties, are from retrievals that include data from the AIRS and AMSU (Advanced Microwave Sounding Unit) suite of instruments on Aqua (e.g., Aumann et al., 2003; Chahine et al., 2006) as well as other datasets (see appendix).

3 Results

A set of 1000 temperature and water vapor reference profiles from July 2003 are randomly selected but obeying the following constraints: these profiles are over the tropical/subtropical oceans [30 S to 30 N], with cloud cover less than 10% and within a sea surface temperature (SST) range of 298 K to 302 K.

For each of these 1000 reference profiles a search is performed to find analogue profiles that are within absolute value thresholds of 1.4 K for temperature and 1.4 gkg^{-1} for water vapor at any vertical level (with respect to the corresponding reference profiles). The search spans a period from 2003 to 2012, but only includes June-July-August (JJA) for each year. These analogue profiles are also over the tropical/subtropical oceans, in (almost) clear sky (cloud cover less than 10 %) and the analogue SST differences are also within 1.4 K. For each of these analogue profiles, the corresponding cloud-cleared (e.g., Susskind et al., 2003) AIRS spectral radiances are selected.

To estimate the impact of CO_2 increase on the observed spectral radiances, the differences between the radiances observed at the location/time of each analogue and the radiances observed at the location/time of the corresponding reference profile are calculated. These differences (that correspond to different reference profiles and different years from 2003 to 2012) are aggregated to provide an estimate of the overall annual mean difference. These differences between the spectral radiances - that are measured at different years and as such reflect different amounts of CO_2 - are compared with theoretical estimates of the radiance impact of CO_2. A key assumption (that is discussed below) is that the annual mean spectral radiance differences corresponding to each reference state are (to first order) not sensitive to the reference state itself for these selected reference profiles.

To estimate the theoretical values, the spectral radiances corresponding to the reference temperature and water vapor profiles are simulated with different values of CO_2 concentration that reflect its mean increase from 2003 to 2012 as measured by the NOAA Mauna Loa station (see appendix). The kCARTA forward model (Strow et al., 1998; DeSouza-Machado et al., 2020) is used to simulate the spectral radiances and is convolved with the AIRS spectral response functions to get theoretical AIRS radiances.

To investigate the uncertainties associated with the temperature and water vapor thresholds used to search for analogues, a preliminary theoretical study of these uncertainties is performed: Using one pair (temperature and water vapor) of reference profiles, 1000 synthetic temperature and water vapor analogues are created by drawing from a normal distribution defined by zero mean and standard deviations of 0.5 K and 0.5 gkg^{-1} (which are close to the values estimated based on the observed

Deleted: Two specific approaches are explored. In experiment A, a single set of individual temperature and water vapor profiles is selected (the reference profiles), and a search is performed for analogues that fit within a specific uncertainty range. In experiment B, to increase the number of samples, this approach is extended to 100 sets of reference profiles, followed by a search for analogues that fit these reference profiles to within a slightly less strict uncertainty range.¶

Moved (insertion) [1]

Deleted: jointly with

Formatted: Font color: Text 1

Deleted: –

Deleted: for details.

Moved (insertion) [2]

Deleted: **3 Experiment A: Single Set of Reference Profiles**¶ For experiment A, a search is performed, from 2005 to 2015, for temperature and water vapor profiles within specific Root-Mean-Square (RMS) difference thresholds, with respect to a set of reference profiles. 148 analogues are selected for a specific set of reference profiles (see appendix for details), corresponding to thresholds of 1.2 K for temperature and SST, and 1.2 gkg^{-1} for water vapor (with cloud cover less than 10 %). For each of these analogue profiles, the corresponding cloud-cleared (e.g., Susskind et al., 2003) AIRS spectral radiances are selected. From the ensemble of 148 analogues, to stay as close to nadir as possible, only spectra measured with scan-angles between -5° and 5° from nadir are selected, which corresponds to six 2005 analogues to estimate the 2005 mean and 18 (unevenly distributed across different years) analogues for all the years between 2006 and 2015. ¶

Deleted: radiances: (1) the

Deleted: radiance mean of the 2005 analogues is calculated, and (2) for spectral radiances for each analogue after 2005radiances

Deleted: each of these analogues and

Deleted: 2005 mean are calculated and used to estimate

Deleted: average

Deleted: effect of CO_2.

Formatted: Font color: Text 1

Deleted: 2005

Deleted: 2005

Deleted: 2015.

Formatted: Font color: Text 1

temperature and water vapor analogues corresponding to the 1000 observed reference profiles) with the constraint that the absolute difference values at any level cannot be larger than the thresholds of 1.4 K and 1.4 $g.kg^{-1}$. Theoretical spectral radiances are calculated for each of these 1000 synthetic analogue pairs of profiles, and these theoretical values are used to estimate the impact of the temperature and water vapor thresholds on the spectral radiances.

Figure 1 compares the theoretical spectral radiance differences due to the annual mean increase of CO_2 (for that reference profile) during this period, with the mean spectral differences between the 1000 (synthetic) analogues and the reference profile. Three specific lines are shown in this context: one that includes all the 1000 synthetic spectral radiances, and two additional ones in which radiance difference outliers which are larger than 0.5 $mWm^{-2}sr^{-1}(cm^{-1})^{-1}$ or 1 $mWm^{-2}sr^{-1}(cm^{-1})^{-1}$ are filtered out. The figure is focused on the 680 to 780 cm^{-1} spectral range where the CO_2 effect is more prominent (see below).

In the spectral region between 680 and 720 cm^{-1} the spectral radiance differences due to temperature and water vapor uncertainties are much smaller than the spectral radiance differences due solely to CO_2 increase, for all the analogue difference lines. Between 720 and around 750 cm^{-1}, although the analogue lines are starting to diverge among themselves in certain regions, their values are still smaller than the CO_2 differences. For values above around 750 cm^{-1} where the CO_2 impact is reduced while the impact of water vapor becomes dominant, the analogue difference lines are of the same order of magnitude as the CO_2 difference lines – although the analogue difference values that are calculated using the filter value of 0.5 $mWm^{-2}sr^{-1}(cm^{-1})^{-1}$ are in certain spectral regions clearly smaller than the CO_2 differences. Given the apparent small impact of these temperature and water vapor uncertainties on the spectral radiances in certain key spectral regions, these results provide a degree of confidence on the methodology.

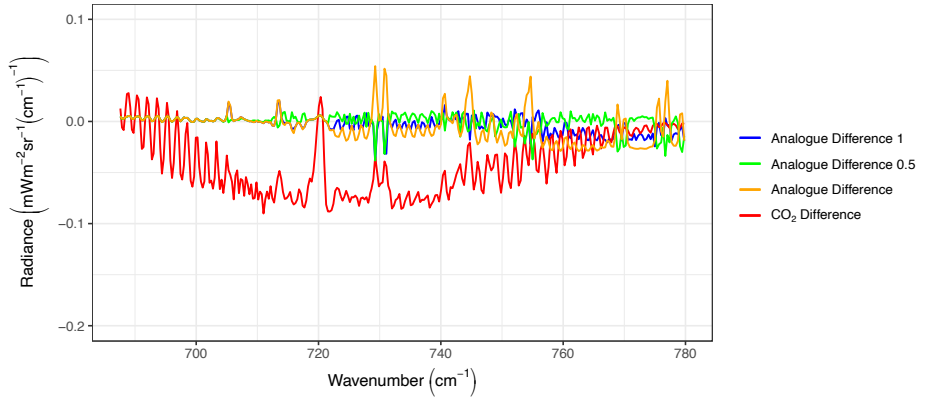

Moved (insertion) [3]

Formatted: Font: 9 pt, Bold

Formatted: Justified

Figure 1: Theoretical spectral radiance differences (in $mWm^{-2}\ sr^{-1}\ (cm^{-1})^{-1}$) due to the annual mean increase of CO_2 during the period from 2003 to 2012 (red line) together with the theoretical mean radiance differences between the 1000 synthetic temperature and water vapor profiles and the reference profile. Three specific lines are shown: one that includes all the 1000 synthetic radiances (orange line), and two additional lines in which radiance difference outliers which are larger than 0.5 $mWm^{-2}sr^{-1}(cm^{-1})^{-1}$ (green line) or 1 $mWm^{-2}sr^{-1}(cm^{-1})^{-1}$ (blue line) are filtered out.

Figure 2 shows the annual mean differences in terms of spectral radiances due to CO_2 increase for the AIRS observations and the theoretical values, together with the standard deviation of the observations. This figure is focused on the 680 to 780 cm^{-1} spectral range, which represents the R-branch of the 15 μm CO_2 band and is a spectral region where the CO_2 signal is particularly significant. In this spectral region, the enhanced absorption within the troposphere, where temperature decreases with height, leads to a reduction of the outgoing radiation. From a broader climate perspective, the reduction of outgoing radiation is behind the increase of global surface temperature that is necessary for the overall climate system to re-establish energy balance at the top of the atmosphere, and as such is a critical component of global warming. During this period, the measured monthly mean CO_2 mole fraction at Mauna Loa increased on average by approximately 2 ppm per year (see appendix).

The theoretical annual **mean differences and** associated **standard deviations** are calculated based on the 1000 reference profiles. These standard deviations are not shown because they are so small that they would be almost imperceptible in the figure. This apparent lack of theoretical sensitivity to the reference states supports the key assumption mentioned above that the annual mean spectral radiance differences corresponding to each reference state are (to first order) not particularly sensitive to the reference state within this specific set of reference profiles.

Figure 2 illustrates that the new methodology leads to observed radiance differences that are close to theory. Despite some noise and a small negative bias in some spectral regions, there is good agreement between theory and observations, with the observations following closely the theoretical impact of increased CO_2. It is noticeable that even in the 750-780 cm^{-1} spectral region, where water vapor plays a large role and larger uncertainties are expected based on figure 1 and the standard deviations, the observations in figure 2 match the theory to a good level of accuracy.

The sensitivity of the observations to different aspects has been analysed. In particular, the observations shown in figure 2 correspond to observed scan-angles between -5° and 5° from nadir (see appendix) and the theoretical radiances are estimated at nadir. To remove outliers and to select analogues that are as close as possible to the reference states, analogues that have absolute radiance differences, as compared to the reference states, that are larger than 0.5 $mWm^{-2}sr^{-1}(cm^{-1})^{-1}$ are filtered out. Overall, the observed spectral radiances shown in figure 2 correspond to about 300 analogues. Results obtained with scan-angles between -10° and 10°, and with outlier filter values of 1 $mWm^{-2}sr^{-1}(cm^{-1})^{-1}$, show no meaningful differences, highlighting the robustness of the methodology.

Given the spatial and temporal variability of CO_2, the lack of accurate knowledge of the CO_2 values for each specific reference state and corresponding analogues leads to uncertainties in the theoretical radiance estimates. A preliminary

Formatted: Font: 9 pt, Bold
Formatted: Font: 9 pt, Bold
Moved (insertion) [4]
Formatted: Caption
Deleted: The theoretical spectral radiances are constructed using the corresponding (observed) monthly mean CO_2 and standard deviation as described in the appendix. For each theoretical a... [1]
Deleted: (between years 2006 to 2015 and the mean 2005 values)
Deleted: (mean and standard deviation of the mean) and th... [2]
Deleted: (mean and standard deviation) given CO_2 uncerta... [3]
Deleted: a wing
Deleted: Note that, during
Moved up [3]: ¶
Moved up [4]: ¶
Moved up [2]: For each of these analogue profiles, the
Deleted: ¶ ... [4]
Deleted: Annual
Deleted: radiance
Deleted: (in $mWm^{-2}\ sr^{-1}\ (cm^{-1})^{-1}$), from the AIRS observa... [5]
Formatted: Font: 9 pt, Bold
Formatted: Font color: Text 1
Formatted: Font color: Text 1
Formatted: Font color: Text 1
Deleted: from theory (red line), and
Deleted: (blue and red shading), between years 2006-201... [6]
Deleted: 1 illustrates that this methodology leads to observ... [7]
Deleted: Following experiment A, only spectra measured w... [8]
Deleted: reference states. This allows to estimate not only t... [9]
Formatted: Font color: Text 1
Deleted: as red shading. Note that the standard deviation is
Deleted: it is
Deleted: , mentioned above, that is made in experiment B.
Deleted: in figure 2
Deleted: 760 to
Deleted: -
Deleted: ,
Deleted: the observations show a clear negative bias in
Deleted: -
Deleted: The theoretical uncertainty associated with the l... [10]
Deleted: ¶ ... [11]

analysis of this uncertainty (not shown) appears to indicate that the observations, in some regions where there are biases, could still be within the theoretical standard deviation range if the CO_2 uncertainties were to be considered explicitly. In fact, using data from the Orbiting Carbon Observatory 2 (Crisp et al., 2004) this analysis leads to theoretical standard deviations of the order of 0.25 $mWm^{-2}sr^{-1}(cm^{-1})^{-1}$ in several channels in the region between 700 and 740 cm^{-1}. This suggests that some of the observational biases could be, at least partly, related to CO_2 uncertainties. Small biases of the radiative transfer model could also potentially be behind some of the differences. A more detailed uncertainty study focused on these two critical aspects is a natural follow up to this work.

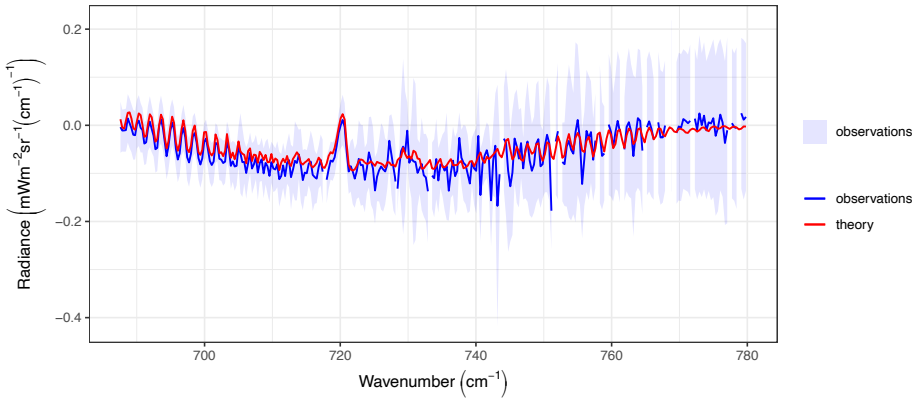

Figure 2: Annual mean radiance differences (in mWm^{-2} sr^{-1} $(cm^{-1})^{-1}$) due to CO_2 increase, from the AIRS observations (blue line) and from theory (red line), and standards deviation for the AIRS observations (blue shading), following the methodology described, and illustrating the direct impact of CO_2 increase on the spectral radiances during the 2003-2012 period (see text for details). Based on observations with scan-angle between -5º and 5º.

Deleted:),
Deleted: for the mean
Deleted: red shading
Deleted: standard deviation
Deleted: in the text for experiment B,

5 Conclusions

We present a direct measurement of the impact of increased atmospheric CO_2 on the spectra of Earth's longwave radiation obtained from space. The approach involves a new methodology to disentangle the impact of CO_2 on the observed longwave spectral radiances, from the effects of temperature and water vapor, in such a way as to provide a direct and more precise comparison with theoretical estimates of the radiance impact of CO_2. The observations obtained using this methodology compare well with theoretical estimates of the direct CO_2 radiative impact on the Earth's longwave spectra.

Deleted:

In the future, variants of this methodology could be used to isolate the observational radiative impact of different physical and chemical properties of the climate system and as such provide a better observational depiction of the Earth's radiative forcing (e.g., Huang et al., 2016; Ramaswamy et al., 2018) and of climate feedbacks.

The stability of the AIRS instrument has been determined to be about one order of magnitude smaller (better) than the climate temporal signal for this spectral region (Strow and DeSouza-Machado, 2020) providing a high level of confidence for the results presented. This work also illustrates the unique and critical role of accurate and stable hyperspectral infrared observations from space in addressing fundamental climate physics questions.

This new methodology can undoubtedly be refined, and its uncertainties better characterized and understood to establish its accuracy and precision more clearly. But as far as the authors are aware, this study represents the first attempt to establish a more precise experimental confirmation from space of the direct effects of CO_2 on longwave spectral radiances. The results (solely based on observations) confirm that the effects of the recent atmospheric CO_2 increase on longwave spectral radiances follow theoretical estimates. As such, these results confirm a critical foundation of the science of global warming.

Appendix: Data and Methods

In this work, the focus is on sets of temperature and water vapor profiles (and the corresponding spectral radiances) that belong to a common physical regime associated with clear sky (or negligible cloud amounts) atmospheric thermodynamics over the tropical and subtropical oceans (from 30° S to 30° N). Figures 3 and 4 compare the mean temperature and water vapor reference profiles with the JJA climatological mean profiles from the AIRS/AMSU retrieval for this regime and illustrate that the reference profiles are indeed representative of the atmospheric thermodynamic climatology of this regime.

AIRS is a hyperspectral sounder on the Aqua spacecraft (Parkinson, 2003) covering the 3.7-15.4 μm infrared spectral region with 2378 channels and spatial resolution of 13.5 km at nadir. AIRS was launched into a 705 km altitude orbit on May 4, 2002, and has been in routine data gathering mode essentially uninterrupted since September 2002. The 1:30 PM ascending node and orbital altitude of the Aqua spacecraft orbit have been accurately maintained (until 2022) and daily (nearly) global coverage is essentially achieved from the ascending and descending orbits. The AIRS radiometric accuracy has been discussed in several studies (e.g., Pagano et al., 2003; Tobin et al., 2006; Aumann et al., 2006). Detailed prelaunch radiometric calibration tests showed that the AIRS radiometric calibration was accurate to within 0.2 K for scene temperatures between 205 K and 310 K (Pagano et al., 2003). As an example, they show that the residual radiometric accuracy compared to an external blackbody at 265 K is between -0.2 and 0.1 K for the vast majority of AIRS channels, and in particular it is between -0.2 and 0 K in the 15 μm spectral region.

AIRS radiances are routinely assimilated in all major global weather prediction systems and are used to retrieve vertical profiles of atmospheric temperature, water vapor, and key atmospheric constituents as well as cloud and surface parameters (e.g., Susskind et al., 2003; Smith and Barnet, 2020).

Deleted: As

Deleted: individual (instantaneous and localized)

Deleted: The AIRS absolute radiometric calibration accuracy is around 0.2 K in brightness temperature (e.g., …

Moved up [1]: Aumann et al.,

Deleted: 2006).

Formatted: Font color: Text 1

Recently, Strow and DeSouza-Machado (2020) confirmed that the AIRS instrument stability for about 400 channels is within 2.10^{-3} $Kyear^{-1}$ in brightness temperature, which is about one order of magnitude smaller than the climate temporal signal in brightness temperature for the spectral region that is investigated in this study. Note that, according to Huang et al. (2022), the trend due to the AIRS instrument spectral shift is also within 2.10^{-3} $Kyear^{-1}$.

The Advanced Microwave Sounding Unit (AMSU) on Aqua is a 15-channel microwave (MW) instrument with 12 temperature sounding channels in the 50-58 GHz oxygen absorption band, that are used to produce an AMSU MW-only retrieved temperature profile dataset (Rosencranz 2001) and are also part of the AIRS/AMSU retrieval.

The atmospheric profiles of temperature and water vapor used in this study are from the AIRS/AMSU retrieval products that are based on level 1 data from AIRS and AMSU, as well as on a neural network retrieval first-guess (Milstein and Blackwell, 2016) that uses the European Centre for Medium-range Weather Forecasts (ECMWF) analyses as the training dataset. In this context, the AIRS/AMSU retrieved profiles of atmospheric temperature and water vapor depend directly on AIRS and AMSU data, and indirectly on the ECMWF data-assimilation system as well as on a variety of observational datasets that are assimilated by ECMWF (e.g., radiosondes, Global Navigation Satellite System (GNSS) Radio Occultation (RO), other infrared (IR) and MW sounders) via a neural network retrieval algorithm. Specifically, version 6 of the AIRS/AMSU retrieval products is used. The standard pressure levels for the retrieved temperature and water vapor profiles are described in:

https://docserver.gesdisc.eosdis.nasa.gov/public/project/AIRS/V7_L2_Standard_Pressure_Levels.pdf.

For temperature, reference profiles and their respective analogues are extracted for both the AIRS/AMSU as well as the AMSU MW-only products. Although the AIRS/AMSU retrievals utilize a large variety of different sources of information about the atmosphere (as described above), the AMSU MW-only retrievals (that are based on the oxygen band and have no dependency on CO_2) are used here as a (somewhat) independent temperature profile dataset to partly validate the methodology.

Figure 3 shows the mean temperature reference profiles for AIRS/AMSU and MW-only retrievals, together with the mean AIRS/AMSU temperature climatology profile for this regime (i.e., the mean of all profiles from JJA 2003 following the constraints referred to above that define this regime). Also shown are the standard deviations of all the analogue profile (from both AIRS/AMSU and MW-only) differences versus the corresponding reference profiles. As mentioned above, this figure illustrates that the reference profiles are representative of this atmospheric thermodynamic regime (as characterized by the AIRS/AMSU climatology). In addition, it shows that the AIRS/AMSU and MW-only reference profiles and their analogues are close to each other. The fact that the analogues have similar characteristics in both the AIRS/AMSU (that uses a variety of sources of information) and the AMSU MW-only retrievals (that are based on the oxygen band) suggests that the analogues appear independent of specific CO_2 assumptions in the retrieval algorithms and in the ECMWF data-assimilation system. Figure 4 shows similar results for the water vapor profiles.

Deleted: combined

Deleted: It is fair to state that

Deleted: and

Deleted: retrieved

Deleted:

Deleted: the

Deleted: ,

Deleted: are analysed

Deleted: also

Deleted: an additional

Formatted: Highlight

Deleted: their temperature profiles in

Deleted: use

Deleted: datasets

Deleted: are in practice

Deleted: .

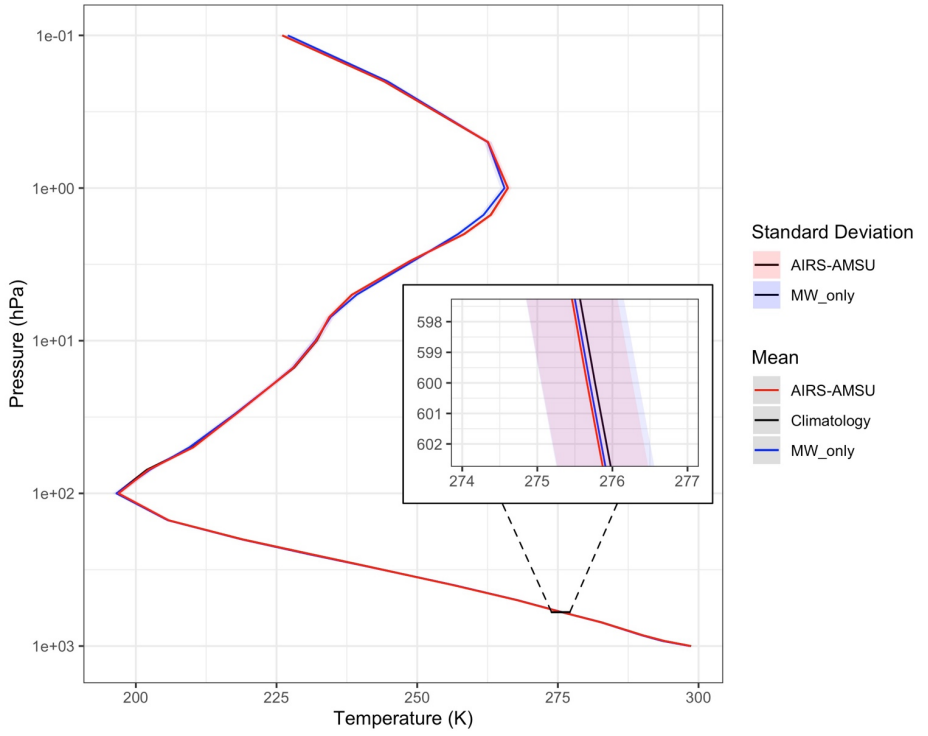

Figure 3. Mean temperature (in K) reference profiles for AIRS/AMSU (red line) and MW-only (blue line) retrievals, together with the mean climatology AIRS/AMSU profile (black line) for this regime. Also shown are the profiles of the standard deviations of all the analogue differences (versus the reference profiles) from both the AIRS/AMSU (red shading) and MW-only (blue shading) analogues.

Note that the temperature and water vapor profile retrieval products discussed above are only used to find analogues and, in this context, other observational estimates of temperature and water vapor could be used for this purpose: e.g., from other IR sounder retrievals such as IASI or the Cross-track Infrared Sounder (CrIS), from other microwave sounder retrievals, or from analysis and re-analysis products. The key reason why AIRS/AMSU temperature and water vapor profiles are used to

Deleted: retrieved

Deleted: mentioned

Deleted: sounders

Deleted: the Infrared Atmospheric Sounding Interferometer (

Deleted:)

Deleted: sounders

Deleted: and AMSU

implement this analogue methodology is the inherent collocation with the AIRS radiance spectra which are directly used in this study.

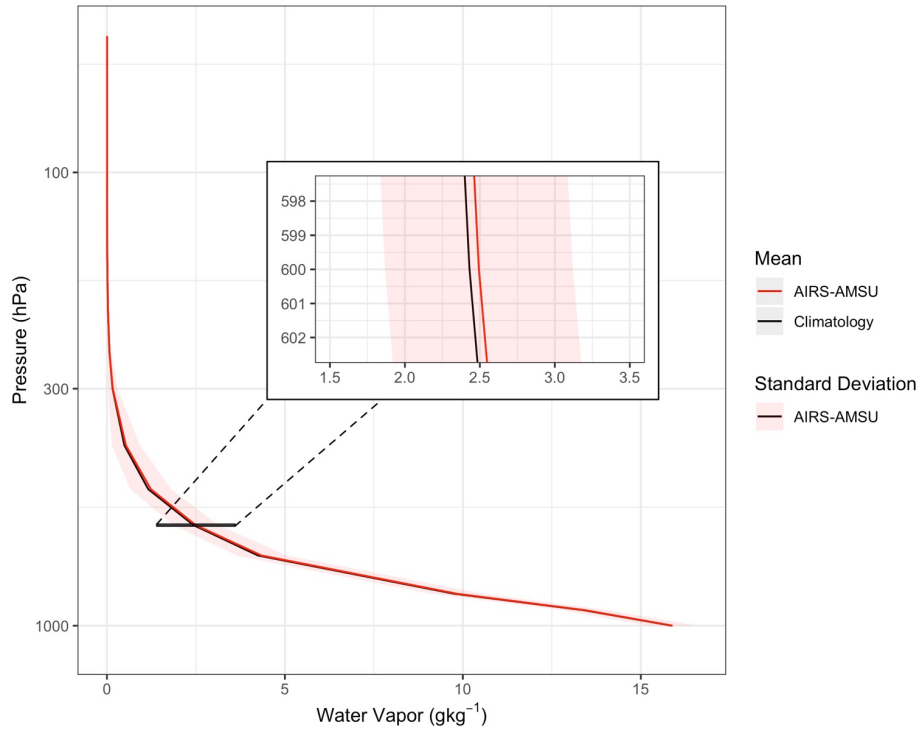

Figure 4. Mean water vapor (in gkg^{-1}) reference profiles for the AIRS/AMSU (red line) and the mean climatology AIRS/AMSU profile (black line) for this regime. Also shown is the profile of the standard deviations of all the analogue differences (versus the reference profiles) from the AIRS/AMSU (red shading) analogues.

Smaller threshold values lead to analogues that are closer to the corresponding reference profiles but to a smaller number of analogues, while larger threshold values lead to analogues that are farther from the corresponding reference profiles but to a larger number of analogues. Based on our initial studies, the specific thresholds of 1.4 K and 1.4 gkg^{-1} that are used in here

Deleted: For experiment A, a few sets of reference profiles of temperature and water vapor were tested. For RMS thresholds of 1 K for temperature and 1 gkg^{-1} for water vapor (mixing ratio) at every vertical level, 7 analogue profiles for a particular set of reference profiles are found (the largest number of analogue profiles attained with this criteria), which is a sample that is too small for a meaningful analysis. Relaxing the thresholds to 1.2 K and 1.2 gkg^{-1}, leads to a much larger number of analogues (148) for that set of reference profiles. These profiles occur in (almost) clear sky (cloud cover less than 10 %) and the sea surface temperature (SST) values are within 1.2 K. This is the set of analogues that is analysed in experiment A. All 148 analogue profiles are from June, July, or August. ¶
For figure 1, the

are a compromise between these extremes. For example, using the same methodology for 1000 reference profiles and thresholds of 1 K and 1 gkg^{-1} does not yield a sufficient number of analogues for precise results to be obtained.

Given the steady increase of global CO_2, the best way to make sure that analogues with significantly different values of CO_2 are selected, is to search for these analogues over several years – ten years from 2003 to 2012 in our study.

The theoretical spectral radiances are calculated for different values of CO_2 that correspond to the mean July CO_2 values for 2003 to 2012, as measured by the National Oceanic and Atmospheric Administration (NOAA) at Mauna Loa (e.g., Thoning et al., 1989). Note that uncertainty associated with the lack of accurate knowledge of CO_2 values for each analogue profile, due to spatial and temporal variability, can lead to noteworthy uncertainties in the theoretical spectral radiances.

Following Huang et al. (2022), to simplify the implementation of the methodology and to circumvent the influence of different viewing zenith angles on the overall results, only spectra measured within scan-angles between -5° and 5° from nadir are presented – although spectra measured within scan-angles between -10° and 10° from nadir are also analysed to evaluate the sensitivity to scan-angle. For consistency, the theoretical radiances are calculated at nadir. Future studies to evaluate the impact of different viewing angles on the results and to increase the observational sample will be performed.

In figure 2, the observational standard deviations grow from values of order 0.01 $mWm^{-2}sr^{-1}(cm^{-1})^{-1}$ close to 700 cm^{-1} to values larger than 0.1 $mWm^{-2}sr^{-1}(cm^{-1})^{-1}$ close to 780 cm^{-1}.

For perspective, when analysing figure 2, note that changes in temperature and water vapor of the order of the ones experienced by the atmosphere during the first 20 years of the 21st century lead to positive theoretical changes in brightness temperature that are fairly constant in this spectral interval, and that correspond to approximately 25% (in absolute value) of the CO_2 theoretical changes in the 720-740 cm^{-1} region, increasing (in percentage) to much higher values toward both the 680 cm^{-1} and the 780 cm^{-1} extremes of the figure (e.g., Huang et al 2022).

These results provide evidence that (i) AIRS has the stability required to address in an accurate and precise manner, climate change questions of the nature described here, and that (ii) space based spectral measurements are becoming of comparable quality to prior spectroscopic estimates. Note that Strow and DeSouza-Machado (2020) estimate that the trend uncertainty due to CO_2 spectroscopy uncertainties is of the order of their estimate for the stability of the AIRS instrument in these channels at around 2.10^{-3} $Kyear^{-1}$. The similarity between the observations and theory in figure 2 further supports this point.

The results presented are for clear sky over the tropical and sub-tropical oceans. Other regions of the globe and physical regimes will be addressed in the future. Performing a similar study that includes cloud effects, to address the all-sky impact, requires overcoming more challenging obstacles both from the observational (analogue) perspective as well as from the theoretical (radiative forward model) perspective.

Code availability: The kCARTA model is available at (SRCv1.18 was used): https://github.com/sergio66/kcarta_gen.

Deleted: three

Deleted: 2005, 2010 and 2015

Deleted: A function is fitted to these three sets of spectral radiances to be able to estimate spectral radiances for any other value of CO_2. Since the actual CO_2 values are not accurately known for each individual analogue profile, the monthly mean observed CO_2 values (at Mauna Loa) of the corresponding month and year are used.Note that

Deleted: The uncertainty associated with the lack of accurate knowledge of CO_2 values for each analogue profile can lead to noteworthy uncertainties in the theoretical spectral radiances. The CO_2 uncertainty for each theoretical analogue (due to CO_2 variability in space and time) is estimated in the following way: from the Orbiting Carbon Observatory-2 (OCO-2) data (Crisp et al., 2004), a value of 1.7 ppm is obtained as an approximate estimate of the spatial standard deviation, and to this value an additional 0.5 ppm is added as a rough estimate of the temporal variability within the June-July-August period.¶

Deleted: 1

Deleted: As mentioned in the main text, only the AIRS observed radiances measured within a scan angle of -5° to 5° are used. To examine the sensitivity to scan-angle selection, results with scan-angles between -10° and 10° from nadir are also analysed for experiment A (not shown), which correspond to 7 analogues for the 2005 mean and 27 analogues for years between 2006 and 2015. Overall, the results with scan-angles between -10° and 10° are fairly similar to figure 1, with a worse negative bias (compared to theory) in the region from 700 to 740 cm^{-1}, and a slightly less negative bias in the region from 760 to 780 cm^{-1}.¶
For experiment B (as in experiment A) to stay as close to nadir as possible, only spectra measured with scan-angles between -5° and 5° from nadir are selected, which leads to a reduction from 100 to 55 reference profiles (states). This is because for 45 of these reference states not a single analogue, for years after 2003, is found within scan-angles of -5° to 5°.¶
For figure 2, to remove outliers and to select analogues that are as close as possible to the reference states, analogues that have absolute radiance differences, as compared to the reference states, that are larger than 0.5 $mWm^{-2}sr^{-1}(cm^{-1})^{-1}$ are filtered out. Results with a larger filter value of 1 $mWm^{-2}sr^{-1}(cm^{-1})^{-1}$ are similar to the ones with 0.5 $mWm^{-2}sr^{-1}(cm^{-1})^{-1}$ from 680 to 740 cm^{-1} but slightly noisier above 740 cm^{-1} where water vapor plays a larger role. Note that the theoretical radiance differences are about 50 times smaller than the filter value in the spectral region 770-780 cm^{-1} where the observational noise is more significant when compared to theory. ¶

Deleted: ¶

Data availability: The AIRS/AMSU version 6 and AMSU MW-only L2 standard products are used for the temperature and water vapor profiles: https://doi.org/10.5067/Aqua/AIRS/DATA201. For AIRS L1B infrared radiances (version 5): https://doi.org/10.5067/YZEXEVN4JGGJ.

Author contributions: JT developed the methodology, performed the analysis, and wrote the manuscript. RCW and HTT implemented the methodology and contributed to the analysis and the manuscript.

Competing interests: The authors declare that they have no conflict of interest.

Financial support: The research described in this manuscript was carried out at the Jet Propulsion Laboratory, California Institute of Technology, under a contract with the National Aeronautics and Space Administration (80NM0018D0004).

Acknowledgements: The authors would like to thank everyone who has been involved in creating the AIRS radiance record. Exciting conversations over the years with several colleagues, including L. Strow, C. Barnet, H. Aumann, S. DeSouza-Machado and X. Huang, are gratefully acknowledged. The authors would also like to thank the two referees for insightful and valuable reviews.

Deleted: 2023

References

Archer, D. and Pierrehumbert, R. (Eds.): The warming papers: The scientific foundation for the climate change forecast. John Wiley & Sons., New York, USA, 432 pp., ISBN: 978-1-405-19616-1, 2011.

Aumann, H.H., et al.: AIRS/AMSU/HSB on the Aqua mission: design, science objectives, data products, and processing systems. IEEE Trans. Geosci. Rem. Sens., 41, 253-264. doi: 10.1109/TGRS.2002.808356, 2003.

Aumann, H.H., Broberg, S., Elliott, D., Gaiser, S. and Gregorich, D.: Three years of atmospheric infrared sounder radiometric calibration validation using sea surface temperatures, J. Geophys. Res.: Atmos., 111, D16S90, doi:10.1029/2005JD006822, 2006.

Brindley, H.E. and Bantges, R.J.: The spectral signature of recent climate change, Current Climate Change Reports, 2, 112–126, doi:10.1007/s40641-016-0039-5, 2016.

Chahine, M.T., Pagano, T.S., Aumann, H.H., Atlas, R., Barnet, C., Blaisdell, J., Chen, L., Divakarla, M., Fetzer, E.J., Goldberg, M. and Gautier, C.: AIRS: Improving weather forecasting and providing new data on greenhouse gases, Bull. Amer. Meteor. Soc., 87, 911–926, doi:10.1175/BAMS-87-7-911, 2006.

Formatted: Font: Times New Roman

Crisp, D., Atlas, R.M., Breon, F.M., Brown, L.R., Burrows, J.P., Ciais, P., Connor, B.J., Doney, S.C., Fung, I.Y., Jacob, D.J. and Miller, C.E.: The orbiting carbon observatory (OCO) mission, Adv. Space Res., 34, 700–709, doi: 10.1016/j.asr.2003.08.062, 2004.

De Longueville, H., Clarisse, L., Whitburn, S., Franco, B., Bauduin, S., Clerbaux, C., Camy-Peyret, C., and Coheur, P.-F.: Identification of short and long-lived atmospheric trace gases from IASI space observations. Geophys. Res. Lett., 48, e2020GL091742, doi. Org/10.1029/2020GL091742, 2021.

DeSouza-Machado, S., Strow, L.L., Motteler, H. and Hannon, S.: kCARTA: a fast pseudo line-by-line radiative transfer algorithm with analytic Jacobians, fluxes, nonlocal thermodynamic equilibrium, and scattering for the infrared, Atmos. Meas. Tech., 13, 323–339, doi:10.5194/amt-13-323-2020, 2020.

Hansen, J., Lacis, A., Rind, D., Russell, G., Stone, P., Fung, I., Ruedy, R. and Lerner, J.: Climate sensitivity: analysis of feedback mechanisms, In: Climate Processes and Climate Sensitivity, AGU Geophysical Monograph, Maurice Ewing volume 5, edited by J.E. Hansen and T. Takahashi, American Geophysical Union, Washington D.C., USA, 29, 130–163, doi:10.1029/GM029p0130, 1984.

Harries, J.E., Brindley, H.E., Sagoo, P.J. and Bantges, R.J.: Increases in greenhouse forcing inferred from the outgoing longwave radiation spectra of the Earth in 1970 and 1997, Nature, 410, 355–357, doi:10.1038/35066553, 2001.

Huang, Y., Tan, X., and Xia, Y.: Inhomogeneous radiative forcing of homogeneous greenhouse gases. J. Geophys. Res. Atmos., 121, 2780–2789, doi:10.1002/2015JD024569, 2016.

Huang, X., Chen, X., Fan, C., Kato, S., Loeb, N., Bosilovich, M., Ham, S.-H., Rose, F.G., and Strow, L.L.: A synopsis of AIRS global-mean clear-sky radiance trends from 2003 to 2020. J. Geophys. Res.: Atmos., 127, e2022JD037598, doi.org/10.1029/2022JD037598, 2022.

Kiehl, J.T.: Satellite detection of effects due to increased atmospheric carbon dioxide, Science, 222, 504–506, doi:10.1126/science.222.4623.504, 1983.

Manabe, S. and Wetherald, R.T.: Thermal equilibrium of the atmosphere with a given distribution of relative humidity, J. Atmos. Sci., 24, 241–259, doi:10.1175/1520-0469(1964)021<0361:TEOTAW>2.0.CO;2, 1967.

Manabe, S. and Wetherald, R.T.: The effects of doubling the CO_2 concentration on the climate of a general circulation model, J. Atmos. Sci., 32, 3–15, doi:10.1175/1520-0469(1975)032<0003:TEODTC>2.0.CO;2, 1975.

Milstein, A.B., and Blackwell, W.J.: Neural network temperature and moisture retrieval algorithm validation for AIRS/AMSU and CrIS/ATMS, J. Geophys. Res. Atmos., 121, 1414–1430, doi:10.1002/2015JD024008, 2016.

Mlynczak, M.G., Daniels, T.S., Kratz, D.P., Feldman, D.R., Collins, W.D., Mlawer, E.J., Alvarado, M.J., Lawler, J.E., Anderson, L.W., Fahey, D.W. and Hunt, L.A.: The spectroscopic foundation of radiative forcing of climate by carbon dioxide, Geophys. Res. Lett., 43, 5318–5325, doi:10.1002/2016GL068837, 2016.

Pagano, T.S., Aumann, H.H., Hagan, D.E., and Overoye, K.: Prelaunch and in-flight radiometric calibration of the Atmospheric Infrared Sounder (AIRS). IEEE Trans. Geosci. Rem. Sens., 41, 265-273. doi: 10.1109/TGRS.2002.808324, 2003.

Formatted: author, Font color: Auto

Parkinson, C.L.: Aqua: An Earth-observing satellite mission to examine water and other climate variables, IEEE Trans. Geosci. Rem. Sens., 41, 173–183, doi:10.1109/TGRS.2002.808319, 2003.

Plass, G.N.: The influence of the 15μ carbon-dioxide band on the atmospheric infra-red cooling rate, Quart. J. Roy. Meteor. Soc., 82, 310–324, doi:10.1002/qj.49708235307, 1956.

Ramanathan, V.: The greenhouse theory of climate change: a test by an inadvertent global experiment. Science, 240, 293-299, DOI:10.1126/science.240.4850.293, 1988.

Ramaswamy, V., Collins, W., Haywood, J., Lean, J., Mahowald, N., Myhre, G., Naik, V., Shine, K.P., Soden, B., Stenchikov, G., and Storelvmo, T.: Radiative Forcing of Climate: The Historical Evolution of the Radiative Forcing Concept, the Forcing Agents and their Quantification, and Applications. Meteor. Monogr., 59, 14.1–14.101, https://doi.org/10.1175/AMSMONOGRAPHS-D-19-0001.1., 2018.

Rosenkranz, P.W.: Retrieval of temperature and moisture profiles from AMSU-A and AMSU-B measurements. IEEE Trans. Geosci. Rem. Sens., 39, 2429-2435, doi:10.1109/36.964979, 2001.

Smith, N. and Barnet, C.D.: CLIMCAPS observing capability for temperature, moisture, and trace gases from AIRS/AMSU and CrIS/ATMS, Atmos. Meas. Tech., 13, 4437–4459, doi:10.5194/amt-13-4437-2020, 2020.

Strow, L.L., Motteler, H.E., Benson, R.G., Hannon, S.E. and De Souza-Machado, S.: Fast computation of monochromatic infrared atmospheric transmittances using compressed look-up tables, J. Quant. Spectrosc. Ra., 59, 481–493, doi:10.1016/S0022-4073(97)00169-6, 1998.

Strow, L.L. and DeSouza-Machado, S.: Establishment of AIRS climate-level radiometric stability using radiance anomaly retrievals of minor gases and sea surface temperature, Atmos. Meas. Tech., 13, 4619–4644, doi:10.5194/amt-13-4619-2020, 2020.

Susskind, J., Barnet, C.D. and Blaisdell, J.M.: Retrieval of atmospheric and surface parameters from AIRS/AMSU/HSB data in the presence of clouds, IEEE Trans. Geosci. Rem. Sens., 41, 390–409, doi:10.1109/TGRS.2002.808236, 2003.

Thoning, K.W., Tans, P.P., Komhyr, W.D.: Atmospheric carbon dioxide at Mauna Loa Observatory: 2. Analysis of the NOAA GMCC data 1974-1985, J. Geophys. Res., 94, 8549–8565, doi:10.1029/JD094iD06p08549, 1989.

Tobin, D. C., et al.: Radiometric and spectral validation of Atmospheric Infrared Sounder observations with the aircraft-based Scanning High-Resolution Interferometer Sounder. J. Geophys. Res., 111, D09S02, doi:10.1029/2005JD006094, 2006.

Whitburn, S., Clarisse, L., Bouillon, M., Safieddine, S., George, M., Dewitte, S., De Longueville, H., Coheur, P.F. and Clerbaux, C.: Trends in spectrally resolved outgoing longwave radiation from 10 years of satellite measurements. npj climate and atmospheric science, 4, 1–8, doi:10.1038/s41612-021-00205-7, 2021.

Page 5: [1] Deleted **Teixeira, Joao** **1/22/24 7:35:00 PM**

Page 5: [2] Deleted **Teixeira, Joao** **1/22/24 7:35:00 PM**

Page 5: [3] Deleted **Teixeira, Joao** **1/22/24 7:35:00 PM**

Page 5: [4] Deleted **Teixeira, Joao** **1/22/24 7:35:00 PM**

Page 5: [5] Deleted **Teixeira, Joao** **1/22/24 7:35:00 PM**

Page 5: [6] Deleted **Teixeira, Joao** **1/22/24 7:35:00 PM**

Page 5: [7] Deleted **Teixeira, Joao** **1/22/24 7:35:00 PM**

Page 5: [8] Deleted **Teixeira, Joao** **1/22/24 7:35:00 PM**

Page 5: [9] Deleted **Teixeira, Joao** **1/22/24 7:35:00 PM**

Page 5: [10] Deleted **Teixeira, Joao** **1/22/24 7:35:00 PM**

Page 5: [11] Deleted **Teixeira, Joao** **1/22/24 7:35:00 PM**